HHS Public Access

Author manuscript

J Invest Dermatol. Author manuscript; available in PMC 2020 February 01.

Published in final edited form as:

J Invest Dermatol. 2019 February ; 139(2): 360–368. doi:10.1016/j.jid.2018.07.030.

Inhibition of Tissue-Nonspecific Alkaline Phosphatase Attenuates Ectopic Mineralization in the *Abcc6*$^{-/-}$ Mouse Model of PXE but not in the *Enpp1* Mutant Mouse Models of GACI

Qiaoli Li[1], **Jianhe Huang**[1], **Anthony B. Pinkerton**[2], **Jose Luis Millan**[2], **BD van Zelst**[3], **Michael A. Levine**[4], **John P. Sundberg**[5], and **Jouni Uitto**[1]

[1]Department of Dermatology and Cutaneous Biology, Sidney Kimmel Medical College, and PXE International Center of Excellence in Research and Clinical Care, Thomas Jefferson University, Philadelphia, PA, USA [2]Sanford-Burnham-Prebys Medical Discovery Institute, La Jolla, CA, USA [3]Department of Clinical Chemistry, Erasmus MC, University Medical Center Rotterdam, Rotterdam, the Netherlands [4]Division of Endocrinology, Children's Hospital of Philadelphia, and University of Pennsylvania Perelman School of Medicine, Philadelphia, PA, USA [5]The Jackson Laboratory, Bar Harbor, ME, USA

Abstract

Pseudoxanthoma elasticum (PXE), a prototype of heritable ectopic mineralization disorders, is caused by mutations in the *ABCC6* gene encoding a putative efflux transporter ABCC6. It was recently demonstrated that the absence of ABCC6-mediated ATP release from the liver, and consequently reduced PPi levels, underlie the pathogenesis of PXE. Given that tissue-nonspecific alkaline phosphatase (TNAP), encoded by *ALPL,* is the enzyme responsible for degrading PPi, we hypothesized that reducing TNAP levels either by genetic or pharmacological means would lead to amelioration of the ectopic mineralization phenotype in the *Abcc6*$^{-/-}$ mouse model of PXE. Thus, we bred *Abcc6*$^{-/-}$ mice to heterozygous *Alpl*$^{+/-}$ mice that display approximately 50% plasma TNAP activity. The *Abcc6*$^{-/-}$*Alpl*$^{+/-}$ double mutant mice showed 52% reduction of mineralization in the muzzle skin compared to the *Abcc6*$^{-/-}$ *Alpl*$^{+/+}$ mice. Subsequently, oral administration of SBI-425, a small molecule inhibitor of TNAP, resulted in 61% reduction of plasma TNAP activity and 58% reduction of mineralization in the muzzle skin of *Abcc6*$^{-/-}$ mice. By contrast, SBI-425 treatment of *Enpp1* mutant mice, another model of ectopic mineralization associated with reduced

Address for Correspondence: Qiaoli Li, Ph.D., Department of Dermatology and Cutaneous Biology, Sidney Kimmel Medical College, PXE International Center of Excellence in Research and Clinical Care, Thomas Jefferson University, 233 S. 10th Street, Suite 431 BLSB, Philadelphia, Pennsylvania 19107, Qiaoli.Li@Jefferson.edu.

CONFLICT OF INTEREST

The authors state no conflict of interest. Anthony B. Pinkerton and Jose Luis Millan are inventors on a patent application covering SBI-425 (PCT WO 2013126608). John P. Sundberg has sponsored research with Takeda, Theravance, and Curadim and does consulting for Bioniz, none of which has any relevance to this project. Michael A. Levine is a member of a Clinical Advisory Board for Inozyme Pharma.

PPi, failed to reduce muzzle skin mineralization. These results suggest that inhibition of TNAP might provide a promising treatment strategy for PXE, a currently intractable disease.

Keywords

Pseudoxanthoma elasticum; ectopic mineralization; mouse model; inorganic pyrophosphate; tissue-nonspecific alkaline phosphatase

INTRODUCTION

Ectopic mineralization - inappropriate biomineralization in soft connective tissues - is a widespread pathological problem encountered frequently during physiological aging and found in several common disorders (obesity, diabetes, chronic kidney disease, etc.) causing significant morbidity and mortality (Giachelli, 1999). In addition, ectopic mineralization is seen in several rare genetic disorders with defined gene defects. Pseudoxanthoma elasticum (PXE), a multisystem disorder with a protean phenotypic spectrum, is one example of a heritable ectopic mineralization disorder. The clinical manifestations in PXE are primarily evident in the skin, eyes, and cardiovascular system (Neldner, 1988; Uitto et al., 2017). PXE is a late-onset and slowly progressive disease with systemic manifestations for which there is no effective treatment.

PXE is caused in most cases by biallelic loss-of-function mutations in the *ABCC6* gene (Bergen et al., 2000; Le Saux et al., 2000; Ringpfeil et al., 2000). The *ABCC6* gene encodes ABCC6, a putative transmembrane efflux transporter protein primarily expressed in the liver (Belinsky and Kruh, 1999; Scheffer et al., 2002). The metabolic features of PXE have been determined to be a consequence of defective ABCC6 transporter activity in hepatocytes (Jiang et al., 2009; Li et al., 2017). It was recently shown that under physiologic conditions ABCC6 mediates adenosine triphosphate (ATP) release from the liver to the extracellular space. Outside the liver, but still within the confines of the liver vasculature, pericellular ATP is rapidly hydrolyzed into adenosine monophosphate and inorganic pyrophosphate (PPi) by ENPP1, an ectonucleotidase (Jansen et al., 2014; Jansen et al., 2013). As a result, plasma levels of PPi are reduced to approximately 30-40% of normal in patients with PXE and in *Abcc6*$^{-/-}$ murine models (Jansen et al., 2014; Jansen et al., 2013; Li et al., 2017). *ENPP1* mutations are associated with type 1 generalized arterial calcification of infancy (GACI) while *ABCC6* mutations are also associated with type 2 GACI, heritable ectopic mineralization disorders in which low or absent levels of PPi are associated with early onset of extensive vascular mineralization that causes significant mortality in infancy (Li et al., 2014a; Nitschke et al., 2012; Rutsch et al., 2003). Collectively, ABCC6-mediated ATP release and subsequent conversion to plasma PPi by ENPP1 links the shared pathogenetic pathway from mutations in the *ABCC6* and *ENPP1* genes to plasma PPi deficiency and eventually ectopic mineralization in PXE and GACI (Uitto et al., 2017).

PPi has been recognized as a potent mineralization inhibitor for four decades (Orriss et al., 2016; Meyer, 1984), and deficiency of PPi levels was recently established as the underlying cause for PXE as a result of *ABCC6* mutations. These results suggest that therapeutics capable of counteracting ectopic mineralization by targeting PPi deficiency could be of use

for treating PXE. One approach towards increasing PPi levels involves inhibition of tissue-nonspecific alkaline phosphatase (TNAP, encoded by the *ALPL* gene), a membrane-bound enzyme that degrades PPi. The early development of *Abcc6*$^{-/-}$ mice has provided a model system to explore potential treatment modalities for PXE (Klement et al., 2005). In this study, two experiments were performed to attempt to inhibit TNAP activity. As a proof of concept, a genetic model, *Abcc6*$^{-/-}$*Alpl*$^{+/-}$ mice, was used to determine the effect of reduced TNAP activity on ectopic mineralization. Subsequently, *Abcc6*$^{-/-}$ mice were treated with SBI-425 (Pinkerton et al., 2018), a small molecule inhibitor of TNAP, to test whether SBI-425 provides sustained and titratable inhibition of TNAP activity and consequently might counteract ectopic mineralization. The results demonstrated that inhibition of TNAP activity attenuated ectopic mineralization in the *Abcc6*$^{-/-}$ mouse model. However, the therapeutic effect of TNAP inhibition was not caused by increased plasma PPi levels, suggesting there are other mechanisms by which TNAP inhibition attenuates ectopic mineralization. Interestingly, inhibition of TNAP activity by SBI-425 had no effect on ectopic mineralization in the *Enpp1*^{asj} and *Enpp1*$^{asj\text{-}2J}$ mutant mouse models of GACI which also display extremely low levels of plasma PPi (Li et al., 2013; Li et al., 2014b).

RESULTS

Reduced TNAP activity attenuated connective tissue mineralization in *Abcc6*$^{-/-}$ mice

To explore the potential efficacy of inhibition of TNAP activity for counteracting ectopic mineralization in PXE, *Abcc6*$^{-/-}$ mice were crossed with *Alpl*$^{+/-}$ mice to generate *Abcc6*$^{-/-}$*Alpl*$^{+/-}$ mice. If reduced TNAP activity in the *Abcc6*$^{-/-}$*Alpl*$^{+/-}$ mice resulted in elevated plasma levels of PPi, a natural substrate of TNAP, it was expected to ameliorate the degree of ectopic mineralization in the *Abcc6*$^{-/-}$ mice. The *Alpl*$^{-/-}$ mice and patients with genetic deficiency of TNAP develop hypophosphatasia, caused by accumulation in the extracellular matrix of PPi, a potent mineralization inhibitor (Fedde et al., 1999; Whyte et al., 2012; Russell, 1965; Russell et al., 1971). Consequently, these mice die during the early postnatal period. As compared to wild type mice, the *Alpl*$^{+/-}$ mice have ~50% plasma TNAP activity but exhibit normal skeletal development. Thus, the *Abcc6*$^{-/-}$ mice were crossed with *Alpl*$^{+/-}$ mice and the corresponding *Abcc6*$^{-/-}$*Alpl*$^{+/+}$ and *Abcc6*$^{-/-}$*Alpl*$^{+/-}$ mice were used to assess the effects of a controlled 50% reduction of TNAP activity on plasma PPi levels and ectopic mineralization. Wild type C57BL/6J mice served as baseline of normal plasma PPi levels and negative controls of ectopic tissue mineralization. All mice were kept on standard control diet and euthanized at 12 weeks of age for analysis.

Mineralization of the dermal sheath of vibrissae in the muzzle skin, an early and reliable biomarker in the overall mineralization process in the *Abcc6*$^{-/-}$ mice, was examined by two independent assays. One piece of muzzle skin was processed for semi-quantitative histopathologic examinations. A mineralization-specific stain, von Kossa, revealed robust mineralization in the dermal sheath of vibrissae in the *Abcc6*$^{-/-}$*Alpl*$^{+/+}$ mice. The *Abcc6*$^{-/-}$*Alpl*$^{+/-}$ mice showed significantly reduced mineralization in the muzzle skin (Fig. 1a). Another piece of muzzle skin was solubilized and the amount of calcium was quantitated using a chemical assay of calcium. The calcium assay showed a significant

reduction of 52% in the amount of calcium in the muzzle skin in the *Abcc6*$^{-/-}$*Alpl*$^{+/-}$ mice (Fig. 1b).

Plasma PLP levels, but not PPi levels, were increased in *Abcc6*$^{-/-}$*Alpl*$^{+/-}$ mice

To further examine the consequences of reduced TNAP activity on ectopic mineralization, PPi levels were determined in plasma of wild type C57BL/6J, *Abcc6*$^{-/-}$*Alpl*$^{+/+}$ and *Abcc6*$^{-/-}$*Alpl*$^{+/-}$ mice. Consistent with previous results (Jansen et al., 2014), the *Abcc6*$^{-/-}$*Alpl*$^{+/-}$ mice had approximately 30% plasma PPi levels of that in wild type mice (Fig. 1c). Reduced TNAP activity in *Abcc6*$^{-/-}$*Alpl*$^{+/-}$ mice did not result in a significance increase in plasma PPi levels (Fig. 1c). The plasma levels of another natural substrate of TNAP, pyridoxal 5'-phosphate (PLP), were also determined. The results demonstrated a significant, 2.4-fold, increase of plasma PLP levels in the *Abcc6*$^{-/-}$*Alpl*$^{+/-}$ mice as compared to *Abcc6*$^{-/-}$*Alpl*$^{+/+}$ mice (Fig. 1d). Therefore, plasma PLP but not PPi levels served as a reliable biomarker for inhibition of TNAP activity.

SBI-425, a prototypic small molecule inhibitor of TNAP, attenuated connective tissue mineralization in *Abcc6*$^{-/-}$ mice

Based on the demonstration in the genetic proof of concept study that reduced TNAP activity attenuated ectopic mineralization in *Abcc6*$^{-/-}$ mice, a treatment trial with SBI-425, a selective and orally bioavailable TNAP inhibitor, was initiated. SBI-425 does not inhibit placental, intestinal, or germ-cell alkaline phosphatase, while demonstrating significantly improved pharmacokinetic profiles as compared to the previously identified chemical inhibitors of TNAP (Pinkerton et al., 2018; Sheen et al., 2015). The ability of SBI-425 to target and inhibit TNAP was previously confirmed in mouse models that overexpress human TNAP in vascular smooth muscle cells and endothelial cells and demonstrated significantly reduced aortic calcification and cardiac hypertrophy, without deleterious effects on skeletal mineralization (Sheen et al., 2015; Romanelli et al., 2017). To investigate the effects of SBI-425 for PXE, the *Abcc6*$^{-/-}$ mice were fed a diet supplemented with SBI-425 at two doses, 7.5 and 75 mg/kg body weight/day, starting at 4 weeks of age followed by an additional 8 weeks. As a result of treatment, plasma TNAP activity was reduced by 61% in mice treated with 75 mg/kg/day SBI-425 with concomitant increase of plasma PLP levels (Fig. 2a).

Histologic examination revealed significant reduction in the muzzle skin calcification in the *Abcc6*$^{-/-}$ mice treated with 75 mg/kg/day SBI-425 (Fig. 3a). The same mice treated with 7.5 mg/kg/day SBI-425 had similar levels of ectopic mineralization to the *Abcc6*$^{-/-}$ mice without treatment. The therapeutic effect of SBI-425 was substantiated by measuring the calcium content in muzzle skin biopsies using a chemical assay. The results confirmed a significant, 58%, reduction in the amount of calcium in the *Abcc6*$^{-/-}$ mice treated with 75 mg/kg/day SBI-425, as compared to the untreated *Abcc6*$^{-/-}$ mice (Fig. 3b).

TNAP inhibition by SBI-425 has no effect on bone microarchitecture in *Abcc6*$^{-/-}$ mice

Because reduced TNAP activity, especially complete loss of TNAP activity, is associated with hypophosphatasia, a heritable disease characterized by defective bone mineralization (Millan and Whyte, 2016; Whyte, 2016), the femurs were dissected from wild type

C57BL/6J and *Abcc6*$^{-/-}$ mice for evaluation of their bone microarchitecture as a result of SBI-425 treatment. The femurs were examined by μCT analysis at the end of the treatment trial (Fig. 4). Marked differences in the bone density and trabecular microarchitecture were noted between the male and female mice, consistent with previous reports (Bouleftour et al., 2014; Pennypacker et al., 2009; Li et al., 2015; Li et al., 2016). Consequently, sex-matched comparisons of the μCT results were performed between wild type, untreated *Abcc6*$^{-/-}$ mice and the same mice fed with 75 mg/kg/day SBI-425. No differences were found between wild type and *Abcc6*$^{-/-}$ mice. SBI-425 treatment in *Abcc6*$^{-/-}$ mice did not result in any appreciable changes to bone microarchitecture (Fig. 4). Quantification of the bone microarchitecture did not show significant differences between control and treated mice across all trabecular bone parameters (Table 2). These results attest to the safety of SBI-425 for TNAP inhibition, at oral doses up to 75 mg/kg/day, without deleterious effects on bone morphometry.

SBI-425 has no effect on connective tissue mineralization in *Enpp1* mutant mice

The *Enpp1*^{asj} and *Enpp1*$^{asj\text{-}2J}$ mutant mice serve as models of GACI (Li et al., 2013; Li et al., 2014b). To test the potential efficacy of 75mg/kg/day dietary SBI-425 in counteracting ectopic mineralization these *Enpp1* mutant mice were used. As compared to *Abcc6*$^{-/-}$ mice which have ~30% plasma PPi levels of wild type mice, the *Enpp1*$^{asj\text{-}2J}$ mice have essentially no plasma PPi due to a spontaneous large deletion and a small insertion in the *Enpp1* gene resulting in complete loss of ENPP1 enzyme activity (Li et al., 2014b). By contrast, the *Enpp1*^{asj} mice carry a missense p.V246D mutation with residual, ~15% of ENPP1 enzymatic activity and lowered plasma PPi levels (Li et al., 2013).

The *Enpp1*^{asj} and *Enpp1*$^{asj\text{-}2J}$ mice were fed with SBI-425 starting at 4 weeks of age and followed for an additional 8 weeks. In addition, some pregnant mothers were treated with SBI-425 during pregnancy and nursing and the *Enpp1* homozygous pups continuing the same treatment until 12 weeks of postnatal life. All mice were analyzed at 12 weeks of age. Increased plasma TNAP activity was observed in the *Enpp1*^{asj} and *Enpp1*$^{asj\text{-}2J}$ mice, suggesting a compensatory mechanism to increase bone formation in the absence of ENPP1 (Mackenzie et al., 2012). As a result of SBI-425 treatment, plasma TNAP activities were significantly reduced accompanied by increased plasma PLP levels (Fig. 2b); however, analysis of calcium content and histology in muzzle skin from these mice showed that SBI-425 treatment failed to reduce the degree of ectopic mineralization (Fig. 3c,d).

DISCUSSION

PXE is the prototype of heritable disorders of ectopic mineralization, a group of autosomal recessive disorders, which also includes generalized arterial calcification of infancy (GACI) and arterial calcification due to CD73 deficiency (ACDC). These conditions have both overlapping and distinctive phenotypic features. GACI is characterized by severe, early-onset mineralization of the cardiovascular system and the majority of children with GACI die from cardiovascular collapse during the first six months after birth (Rutsch et al., 2008). By contrast, ACDC is a late-onset mineralization disorder that primarily affects the arteries of the lower extremities and periarticular ligaments (St Hilaire et al., 2011). Mutations in the

ABCC6 gene cause the classic form of PXE and type 2 GACI, while *ENPP1* mutations cause type 1 GACI. Significant recent progress has been made in understanding the pathomechanistic details of ectopic mineralization in these conditions, and this information has now provided a platform to develop treatments for PXE (Uitto et al., 2017). A particularly intriguing recent observation is that release of ATP from hepatocytes to the circulation is dependent on functional ABCC6, and in the absence of ABCC6 transporter activity, as in PXE, the extracellular pool of ATP is reduced and consequently less plasma PPi is generated by ENPP1 hydrolysis. Recent studies indicated that a unifying pathomechanistic feature in PXE, GACI and ACDC involves reduction in PPi levels allowing ectopic mineralization in the peripheral tissues to ensue (Uitto et al., 2017).

PPi levels are regulated by the opposing actions of ENPP1, which generates PPi, and TNAP, which degrades PPi. Since PPi is a powerful anti-mineralization factor, in this study we tested the hypothesis that inhibition of TNAP activity would increase plasma PPi levels and thereby counteract ectopic mineralization in a mouse model of PXE. A genetic model, $Abcc6^{-/-}Alpl^{+/-}$ mice with ~50% reduction of plasma TNAP activity showed significant inhibition of mineralization. To titrate the level of TNAP activity required for inhibition of ectopic mineralization in $Abcc6^{-/-}$ mice, subsequent studies tested two different doses of a small molecule inhibitor of TNAP, SBI-425, which has been shown to reduce vascular mineralization while not adversely affecting bone mineralization in mouse models overexpressing human TNAP (Sheen et al., 2015). The $Abcc6^{-/-}$ mice treated with 75 mg/kg/day SBI-425 demonstrated 61% reduced plasma TNAP activity and ectopic mineralization in the muzzle skin while the same mice treated with 7.5 mg/kg/day SBI-425 did not. The therapeutic effect of SBI-425 did not cause deleterious consequences to the femoral bone in the treated mice. While significant reduction of ectopic mineralization was noted in $Abcc6^{-/-}$ mice either via genetics or pharmacological means for inhibition of TNAP, distinct mineralization was still present, indicating that reduction of TNAP activity up to 61% of the wild type level is not sufficient to completely arrest ectopic mineralization. The early postnatal lethality of the homozygous $Alpl^{-/-}$ mice prevented us to investigate whether a more drastic decrease of TNAP activity, <1% of wild type level, would have more pronounced therapeutic effects in $Abcc6^{-/-}$ mice (Fedde et al., 1999). In addition, though two different doses of SBI-425 was tested for titration, the efficacy for inhibition of TNAP activity did not achieve as high as 95% as we had anticipated for at the planning phase of this study. Further studies might require higher doses for more drastic reduction in TNAP activity and complete mineralization arrest. Please note that the investigational drug, the dose at 75 mg/kg/day and the $Abcc6^{-/-}$ mouse model for PXE in this study mirrors those in another study (Ziegler et al., 2017). Combined results of these independent and complementary studies suggested that inhibition of TNAP by SBI-425 could be turned into a viable approach for treatment of patients with PXE.

Whereas $Abcc6^{-/-}$ mice had decreased plasma PPi concentrations compared to wild type mice, reduced TNAP activity did not significantly increase plasma PPi concentrations as we initially anticipated, potentially highlighting the contribution of other mechanisms, independent of PPi, to the therapeutic effect of TNAP inhibition on attenuation of ectopic mineralization. . Furthermore, in earlier studies where plasma TNAP levels were genetically increased by 10 to 15-fold, plasma PPi levels were not decreased (Narisawa et al., 2013;

Sheen et al., 2015; Savinov et al., 2015). Therefore, plasma PPi levels are not a reliable marker for tracking phenotypic improvement. In this context, the levels of PLP, another physiological substrate for TNAP can be used reliably as a marker of therapeutic benefit (Whyte et al., 2012).

To investigate whether SBI-425 treatment has broader applications beyond PXE, the *Enpp1*^{asj} and *Enpp1*$^{asj\text{-}2J}$ mice, models for GACI, were also treated with SBI-425. Previous studies suggested that three TNAP compounds, unrelated to SBI-425, inhibited TNAP activity and suppressed mineralization in cultured vascular smooth muscle cells derived from *Enpp1*$^{-/-}$ mice (Narisawa et al., 2007). Interestingly, SBI-425 administration at 75 mg/kg/day in both *Enpp1*^{asj} and *Enpp1*$^{asj\text{-}2J}$ mice postnatally or prenatally did not affect the degree of ectopic mineralization. The lack of therapeutic effect of SBI-425 in the context of *ENPP1* mutations could be at least partially explained by distinct pathophysiology of ABCC6 and ENPP1 in preventing ectopic mineralization under physiologic conditions. ENPP1 is the principal enzyme for generation of PPi by ATP hydyolysis. Upstream of ENPP1, ABCC6-mediated ATP release from hepatocytes is the main source of circulating PPi (Jansen et al., 2014). The work by us and others suggest that reduced PPi levels is the major factor leading to ectopic mineralization in PXE, but there might be an alternative, as yet unknown mechanism, independent of PPi, by which ABCC6 prevents ectopic mineralization under physiologic conditions (Zhao et al., 2017; Pomozi et al., 2017). Recent observations suggest that ABCC6 is also involved in extracellular nucleotide metabolism, suggesting a central role for ABCC6 in purinergic signaling in the development of ectopic mineralization (Kauffenstein et al., 2018).

Taken together, ectopic mineralization in PXE can be attenuated by inhibition of TNAP activity genetically or pharmacologically. The lack of restoration of plasma PPi levels does not explain why inhibition of TNAP activity results in attenuation of ectopic mineralization in PXE. Nevertheless, the results derived from the preclinical mouse studies suggest that inhibition of TNAP activity could reduce or slow down progression of the devastating consequences in patients with PXE. The mechanisms by which TNAP inhibition resulted in attenuation of ectopic mineralization in PXE but not in GACI remains unexplained. In this context, TNAP inhibition could be considered for other ectopic mineralization conditions only after careful testing in appropriate model systems.

MATERIALS AND METHODS

Mice and breeding

The *Abcc6*^{tm1JfK} mouse was developed by targeted ablation of the *Abcc6* gene (this mouse is referred to as *Abcc6*$^{-/-}$) (Klement et al., 2005). *Abcc6*$^{-/-}$ mice were made congenic by backcrossing heterozygous mice for 10 generations with wild type C57BL/6J mice (The Jackson Laboratory, Bar Harbor, ME). The *Alpl*$^{+/-}$ mice (*Alpl*^{tm1Jlm}) were obtained from Sanford-Burnham-Prebys Medical Discovery Institute (Fedde et al., 1999) and subsequently backcrossed with C57BL/6J mice for four generations. Compound *Abcc6* and *Alpl* mice were generated by intercrossing *Abcc6*$^{-/-}$ mice with *Alpl*$^{+/-}$ mice. The C57BL/6J-*Enpp1*^{asj}/GrsrJ and BALB/cJ-*Enpp1*$^{asj\text{-}2J}$/GrsrJ mice were obtained from The Jackson Laboratory. These *Enpp1* mutant mice are referred in this publication as the *Enpp1*^{asj} and *Enpp1*$^{asj\text{-}2J}$

mouse, respectively (Li et al., 2013; Li et al., 2014b). The wild type, heterozygous, and homozygous mice were generated from heterozygous matings. The C57BL/6J mice serve as wild type controls for *Abcc6*$^{-/-}$ and *Enpp1*^{asj} mice while BALB/cJ mice serve as wild type controls for *Enpp1*$^{asj\text{-}2J}$ mice. All mice were maintained a standard rodent diet (Lab Diet 5010; PMI Nutrition, Brentwood, MO, USA). All protocols were approved by the Institutional Animal Care and Use Committee of Thomas Jefferson University.

Experimental design and treatments

In the proof of concept genetic study, the C57BL/6J, *Abcc6*$^{-/-}$*Alpl*$^{+/+}$, and *Abcc6*$^{-/-}$*Alpl*$^{+/-}$ mice were fed a control diet throughout the experiments. At 12 weeks of age, these mice were euthanized for analysis. In the TNAP inhibitor SBI-425 treatment experiments, mice were divided into eleven groups (A to K) based on their *Abcc6* or *Enpp1* genotype and treatment regiments (Table 1). Four-week old wild type, *Abcc6*$^{-/-}$, *Enpp1*^{asj}, and *Enpp1*$^{asj\text{-}2J}$ mice were placed on either control diet or experimental diet supplemented with 0.003% or 0.03% SBI-425 and maintained on the same treatment regimen for an additional 8 weeks. The doses correspond to 7.5 or 75 mg/kg body weight/day SBI-425, assuming that a 20 g mouse consumes 5 g food per day. Groups G and K are *Enpp1*^{asj} and *Enpp1*$^{asj\text{-}2J}$ mice, respectively, fed a SBI-425 containing diet (75 mg/kg/day) to the pregnant mothers and continuing the same treatment in pups until pups became 12 weeks of age. All mice were euthanized at 12 weeks of age for analysis.

Histopathological analysis

Muzzle skin biopsies (left side) from euthanized mice were collected and processed for histology. Tissue sections were stained with von Kossa using standard procedures.

Chemical quantitation of calcium

To quantify the mineral deposition in mouse tissues, muzzle skin biopsies (right side) were harvested and decalcified with 1.0 mol/L HCl for 48 hours at room temperature. Solubilized calcium was then determined by colorimetric analysis using the *o*'-cresolphthalein complexone method (calcium (CPC) LiquiColor; Stanbio Laboratory, Boerne, TX). The values were normalized to tissue weight.

Plasma inorganic pyrophosphate assay

Whole blood was collected by cardiac puncture into test tubes containing 100 μL CTAD and stored at room temperature after addition of 10 μL 15% trisodium EDTA (Sigma-Aldrich, St. Louis, MO). After centrifugation, plasma was depleted of platelets by filtration through a Centrisart I 300-kDa mass cutoff filter (Sartorius, New York, NY, USA), and stored at −80°C until further processing. PPi in plasma was measured by an enzymatic reaction using ATP sulfurylase to convert PPi into ATP in the presence of excess adenosine 5'-phosphosulfate (Sigma-Aldrich), a methodology adopted world-wide as described previously (Li et al., 2017; Jansen et al., 2014; Dedinszki et al., 2017; Pomozi et al., 2017; Bauer et al., 2018).

Plasma TNAP activity and PLP assays

In the proof of concept genetic study, the platelet-free plasma was used for determination of PLP levels by a stable isotope dilution LC-ESI-MS/MS method (van Zelst and de Jonge, 2012). In the TNAP inhibitor SBI-425 treatment experiments, heparin plasma was collected for determination of alkaline phosphatase activity using a colorimetric kit from Abcam (Cambridge, MA).

Microcomputed tomography

Microarchitecture of the distal trabecular bone and midshaft region of the right femur was analyzed. A 1.2 mm-thick region located proximal to the distal growth plate of femur was scanned at a 6 μm resolution using the micro-computed tomography (μCT) system (μCT35; Scanco Medical AG, Bassersdorf, Switzerland). The microstructural parameters were obtained through three-dimensional reconstruction and segmentation (using a Gaussian filter and a global threshold of 3685 Hounsfield units) using the manufacturer-provided software.

Statistical analysis

The data were analyzed using multivariable linear regression with the predictor of sex and treatment and their interactions for each group. Statistical significance was reached with $p < 0.05$. All statistical computations were completed using R version 3.5.0 software.

ACKNOWLEDGMENTS

This study was supported by NIH/NIAMS grants R01AR055225 (JU), K01AR064766 (QL), and R01AR072695 (JU and QL). The authors acknowledge Penn Center for Musculoskeletal Disorders, supported by NIH/NIAMS P30AR050950, for assistance in analysis of bone morphometry. The authors thank Dian Wang, Ida Joely Jacobs, Koen van de Wetering, Diana Li, Wei-Ju Tseng, and Tingting Zhan for assistance. Carol Kelly helped in manuscript preparation.

Abbreviations:

Asj	ages with stiffened joints
GACI	generalized arterial calcification of infancy
PLP	pyridoxal 5’-phosphate
PPi	inorganic pyrophosphate
PXE	pseudoxanthoma elasticum
TNAP	tissue-nonspecific alkaline phosphatase

REFERENCES

Bauer C, le Saux O, Pomozi V, Aherrahrou R, Kriesen R, Stolting S, et al. Etidronate prevents dystrophic cardiac calcification by inhibiting macrophage aggregation. Sci Rep 2018;8:5812. [PubMed: 29643466]

Belinsky MG, Kruh GD. MOAT-E (ARA) is a full-length MRP/cMOAT subfamily transporter expressed in kidney and liver. Br J Cancer 1999;80:1342–9. [PubMed: 10424734]

Bergen AA, Plomp AS, Schuurman EJ, Terry S, Breuning M, Dauwerse H, et al. Mutations in ABCC6 cause pseudoxanthoma elasticum. Nat Genet 2000;25:228–31. [PubMed: 10835643]

Bouleftour W, Boudiffa M, Wade-Gueye NM, Bouet G, Cardelli M, Laroche N, et al. Skeletal development of mice lacking bone sialoprotein (BSP)--impairment of long bone growth and progressive establishment of high trabecular bone mass. PLoS One 2014;9:e95144. [PubMed: 24816232]

Dedinszki D, Szeri F, Kozak E, Pomozi V, Tokesi N, Mezei TR, et al. Oral administration of pyrophosphate inhibits connective tissue calcification. EMBO Mol Med 2017;9:1463–70. [PubMed: 28701330]

Fedde KN, Blair L, Silverstein J, Coburn SP, Ryan LM, Weinstein RS, et al. Alkaline phosphatase knock-out mice recapitulate the metabolic and skeletal defects of infantile hypophosphatasia. J Bone Miner Res 1999;14:2015–26. [PubMed: 10620060]

Giachelli CM. Ectopic calcification: gathering hard facts about soft tissue mineralization. Am J Pathol 1999;154:671–5. [PubMed: 10079244]

Jansen RS, Kucukosmanoglu A, de Haas M, Sapthu S, Otero JA, Hegman IE, et al. ABCC6 prevents ectopic mineralization seen in pseudoxanthoma elasticum by inducing cellular nucleotide release. Proc Nat Acad Sci USA 2013;110:20206–11. [PubMed: 24277820]

Jansen RS, Duijst S, Mahakena S, Sommer D, Szeri F, Varadi A, et al. ABCC6-mediated ATP secretion by the liver is the main source of the mineralization inhibitor inorganic pyrophosphate in the systemic circulation-brief report. Arterioscler Thromb Vasc Biol 2014;34:1985–9. [PubMed: 24969777]

Jiang Q, Endo M, Dibra F, Wang K, Uitto J. Pseudoxanthoma elasticum is a metabolic disease. J Invest Dermatol 2009;129:348–54. [PubMed: 18685618]

Kauffenstein G, Yegutkin GG, Khiati S, Pomozi V, Le Saux O, Leftheriotis G, et al. Alteration of extracellular nucleotide metabolism in pseudoxanthoma elasticum. J Invest Dermatol 2018;10.1016/j.jid.2018.02.023.

Klement JF, Matsuzaki Y, Jiang QJ, Terlizzi J, Choi HY, Fujimoto N, et al. Targeted ablation of the *Abcc6* gene results in ectopic mineralization of connective tissues. Mol Cell Biol 2005;25:8299–310. [PubMed: 16135817]

Le Saux O, Urban Z, Tschuch C, Csiszar K, Bacchelli B, Quaglino D, et al. Mutations in a gene encoding an ABC transporter cause pseudoxanthoma elasticum. Nat Genet 2000;25:223–7. [PubMed: 10835642]

Li Q, Guo H, Chou DW, Berndt A, Sundberg JP, Uitto J. Mutant *Enpp1*^{asj} mouse as a model for generalized arterial calcification of infancy. Dis Model Mech 2013;6:1227–35. [PubMed: 23798568]

Li Q, Brodsky JL, Conlin L, Pawel B, Glatz A, Gafni RI, et al. Mutations in the *ABCC6* gene as a cause of generalized arterial calcification of infancy: Genotypic overlap with pseudoxanthoma elasticum. J Invest Dermatol 2014a;134:658–65. [PubMed: 24008425]

Li Q, Pratt CH, Dionne LA, Fairfield H, Karst SY, Sundberg JP, et al. Spontaneous *asj-2J* mutant mouse as a model for generalized arterial calcification of infancy: A large deletion/insertion mutation in the *Enpp1* gene. PLOS One 2014b;9:e113542. [PubMed: 25479107]

Li Q, Sundberg JP, Levine MA, Terry SF, Uitto J. The effects of bisphosphonates on ectopic soft tissue mineralization caused by mutations in the *ABCC6* gene. Cell Cycle 2015;14:1082–9. [PubMed: 25607347]

Li Q, Kingman J, Sundberg JP, Levine MA, Uitto J. Dual effects of bisphosphonates on ectopic skin and vascular soft tissue mineralization versus bone microarchitecture in a mouse model of generalized arterial calcification of infancy. J Invest Dermatol 2016;136:275–83. [PubMed: 26763447]

Li Q, Kingman J, van de Wetering K, Tannouri S, Sundberg JP, Uitto J. Abcc6 knockout rat model highlights the role of liver in PPi homeostasis in pseudoxanthoma elasticum. J Invest Dermatol 2017;137:1025–32. [PubMed: 28111129]

Mackenzie NC, Zhu D, Milne EM, van 't Hof R, Martin A, Darryl Quarles L, et al. Altered bone development and an increase in FGF-23 expression in *Enpp1*$^{-/-}$ mice. PloS One 2012;7:e32177. [PubMed: 22359666]

Meyer JL. Can biological calcification occur in the presence of pyrophosphate? Arch Biochem Biophys 1984;231:1–8. [PubMed: 6326671]

Millan JL, Whyte MP. Alkaline phosphatase and hypophosphatasia. Calcif Tissue Int 2016;98:398–416. [PubMed: 26590809]

Narisawa S, Harmey D, Yadav MC, O'Neill WC, Hoylaerts MF, Millan JL. Novel inhibitors of alkaline phosphatase suppress vascular smooth muscle cell calcification. J Bone Miner Res 2007;22:1700–10. [PubMed: 17638573]

Narisawa S, Yadav MC, Millan JL. In vivo overexpression of tissue-nonspecific alkaline phosphatase increases skeletal mineralization and affects the phosphorylation status of osteopontin. J Bone Miner Res 2013;28:1587–98. [PubMed: 23427088]

Neldner KH. Pseudoxanthoma elasticum. Clin Dermatol 1988;6:1–159.

Nitschke Y, Baujat G, Botschen U, Wittkampf T, du Moulin M, Stella J, et al. Generalized arterial calcification of infancy and pseudoxanthoma elasticum can be caused by mutations in either *ENPP1* or *ABCC6*. Am J Hum Genet 2012;90:25–39. [PubMed: 22209248]

Orriss IR, Arnett TR, Russell RG. Pyrophosphate: a key inhibitor of mineralisation. Curr Opin Pharmacol 2016;28:57–68. [PubMed: 27061894]

Pennypacker B, Shea M, Liu Q, Masarachia P, Saftig P, Rodan S, et al. Bone density, strength, and formation in adult cathepsin K (−/−) mice. Bone 2009;44:199–207. [PubMed: 18845279]

Pinkerton AB, Sergienko E, Bravo Y, Dahl R, Ma CT, Sun Q, et al. Discovery of 5-((5-chloro-2-methoxyphenyl)sulfonamido)nicotinamide (SBI-425), a potent and orally bioavailable tissue-nonspecific alkaline phosphatase (TNAP) inhibitor. Bioorg Med Chem Lett 2018;28:31–4. [PubMed: 29174347]

Pomozi V, Brampton C, van de Wetering K, Zoll J, Calio B, Pham K, et al. Pyrophosphate supplementation prevents chronic and acute calcification in ABCC6-deficient mice. Am J Pathol 2017;187:1258–72. [PubMed: 28416300]

Ringpfeil F, Lebwohl MG, Christiano AM, Uitto J. Pseudoxanthoma elasticum: mutations in the MRP6 gene encoding a transmembrane ATP-binding cassette (ABC) transporter. Proc Natl Acad Sci U S A 2000;97:6001–6. [PubMed: 10811882]

Romanelli F, Corbo A, Salehi M, Yadav MC, Salman S, Petrosian D, et al. Overexpression of tissue-nonspecific alkaline phosphatase (TNAP) in endothelial cells accelerates coronary artery disease in a mouse model of familial hypercholesterolemia. PLoS One 2017;12:e0186426. [PubMed: 29023576]

Russell RG. Excretion of inorganic pyrophosphate in hypophosphatasia. Lancet 1965;2:461–4. [PubMed: 14337825]

Russell RG, Bisaz S, Donath A, Morgan DB, Fleisch H. Inorganic pyrophosphate in plasma in normal persons and in patients with hypophosphatasia, osteogenesis imperfecta, and other disorders of bone. J Clin Invest 1971;50:961–9. [PubMed: 4324072]

Rutsch F, Ruf N, Vaingankar S, Toliat MR, Suk A, Hohne W, et al. Mutations in *ENPP1* are associated with 'idiopathic' infantile arterial calcification. Nature Genet 2003;34:379–81. [PubMed: 12881724]

Rutsch F, Boyer P, Nitschke Y, Ruf N, Lorenz-Depierieux B, Wittkampf T, et al. Hypophosphatemia, hyperphosphaturia, and bisphosphonate treatment are associated with survival beyond infancy in generalized arterial calcification of infancy. Circ Cardiovasc Genet 2008;1:133–40. [PubMed: 20016754]

Savinov AY, Salehi M, Yadav MC, Radichev I, Millan JL, Savinova OV. Transgenic overexpression of tissue-nonspecific alkaline phosphatase (TNAP) in vascular endothelium results in generalized arterial calcification. J Am Heart Assoc 2015;4.

Scheffer GL, Hu X, Pijnenborg AC, Wijnholds J, Bergen AA, Scheper RJ. MRP6 (ABCC6) detection in normal human tissues and tumors. Lab Invest 2002;82:515–8. [PubMed: 11950908]

Sheen CR, Kuss P, Narisawa S, Yadav MC, Nigro J, Wang W, et al. Pathophysiological role of vascular smooth muscle alkaline phosphatase in medial artery calcification. J Bone Miner Res 2015;30:824–36. [PubMed: 25428889]

St Hilaire C, Ziegler SG, Markello TC, Brusco A, Groden C, Gill F, et al. *NT5E* mutations and arterial calcifications. N Engl J Med 2011;364:432–42. [PubMed: 21288095]

Uitto J, Van de Wetering K, Varadi A, Terry SF. Novel insights into pathomechanisms and treatment development in heritable ectopic mineralization disorders. Summary of the PXE International Biennial Research Symposium. J Invest Dermatol 2017;137:790–5. [PubMed: 28340679]

van Zelst BD, de Jonge R. A stable isotope dilution LC-ESI-MS/MS method for the quantification of pyridoxal-5'-phosphate in whole blood. J Chromatogr B Analyt Technol Biomed Life Sci 2012;903:134–41.

Whyte MP, Greenberg CR, Salman NJ, Bober MB, McAlister WH, Wenkert D, et al. Enzyme-replacement therapy in life-threatening hypophosphatasia. N Engl J Med 2012;366:904–13. [PubMed: 22397652]

Whyte MP. Hypophosphatasia - aetiology, nosology, pathogenesis, diagnosis and treatment. Nat Rev Endocrinol 2016;12:233–46. [PubMed: 26893260]

Zhao J, Kingman J, Sundberg JP, Uitto J, Li Q. Plasma PPi deficiency is the major, but not the exclusive, cause of ectopic mineralization in an Abcc6(−/−) mouse model of PXE. J Invest Dermatol 2017;137:2336–43. [PubMed: 28652107]

Ziegler SG, Ferreira CR, MacFarlane EG, Riddle RC, Tomlinson RE, Chew EY, et al. Ectopic calcification in pseudoxanthoma elasticum responds to inhibition of tissue-nonspecific alkaline phosphatase. Sci Transl Med 2017;9.

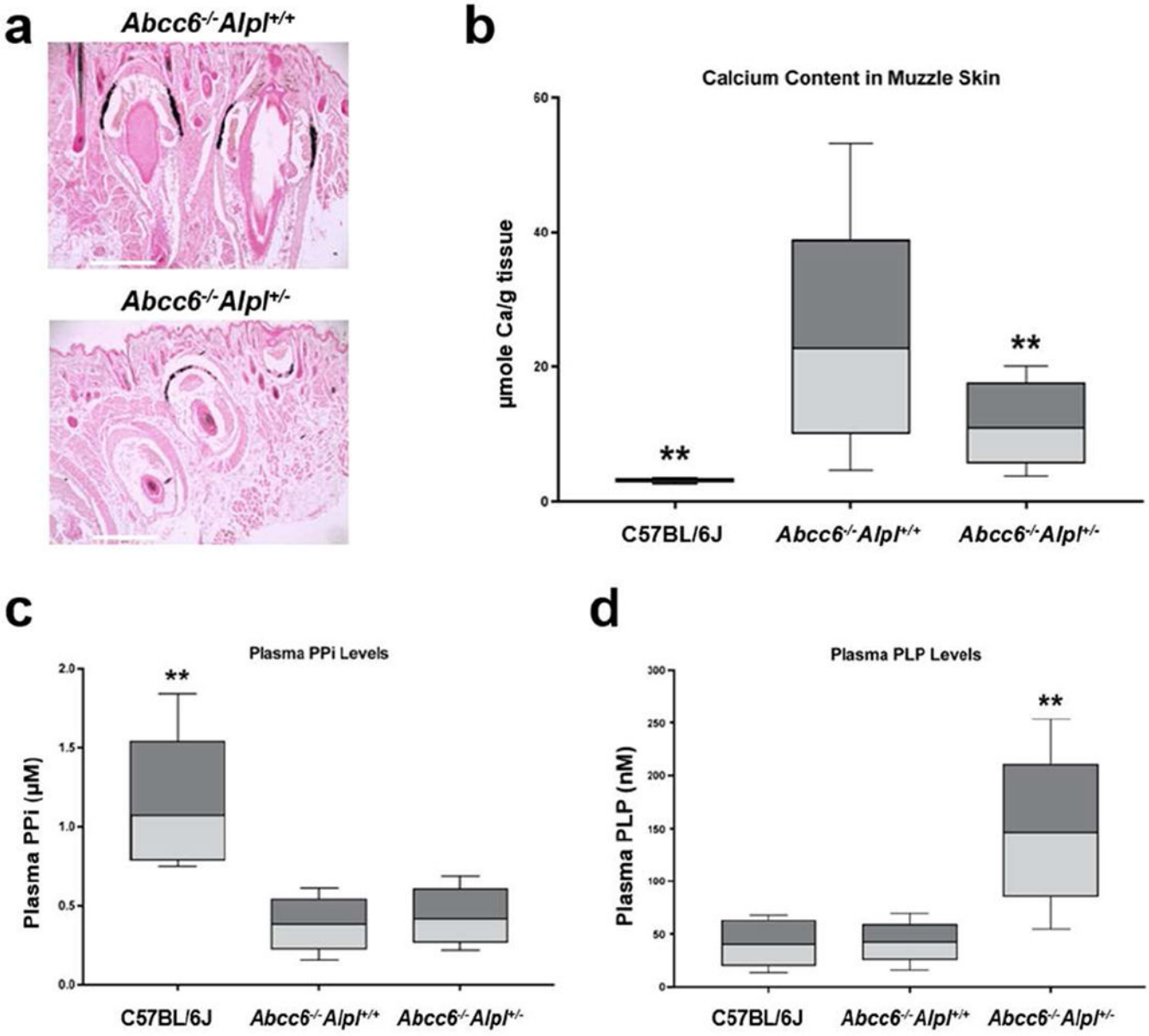

Figure 1. Genetic proof of concept study demonstrated that reduced TNAP activity in the *Alpl*$^{+/-}$ mice inhibited ectopic connective tissue mineralization in the *Abcc6*$^{-/-}$ mice.

(a) Muzzle skin biopsies were processed for histopathology followed by von Kossa stains. The *Abcc6*$^{-/-}$*Alpl*$^{+/-}$ mice (lower panel) developed less ectopic mineralization of the dermal sheath of vibrissae in the muzzle skin compared to *Abcc6*$^{-/-}$*Alpl*$^{+/+}$ mice (upper panel); (b) The amount of calcium in the muzzle skin of *Abcc6*$^{-/-}$*Alpl*$^{+/-}$ mice was significantly decreased as compared to *Abcc6*$^{-/-}$*Alpl*$^{+/+}$ mice; (c) Plasma PPi levels in the *Abcc6*$^{-/-}$*Alpl*$^{+/+}$ mice were 30% of that in wild type mice; however, plasma PPi levels in the *Abcc6*$^{-/-}$*Alpl*$^{+/-}$ mice were not statistically different from that in the *Abcc6*$^{-/-}$ Alpl$^{+/-}$ mice; (d) Plasma levels of PLP were significantly increased in the *Abcc6*$^{-/-}$*Alpl*$^{+/-}$ mice. Values were expressed as mean ± SD; n = 12 - 15 mice per group. $^{**}p < 0.01$, compared with *Abcc6*$^{-/-}$*Alpl*$^{+/+}$ mice. Scale bar, 0.4 mm.

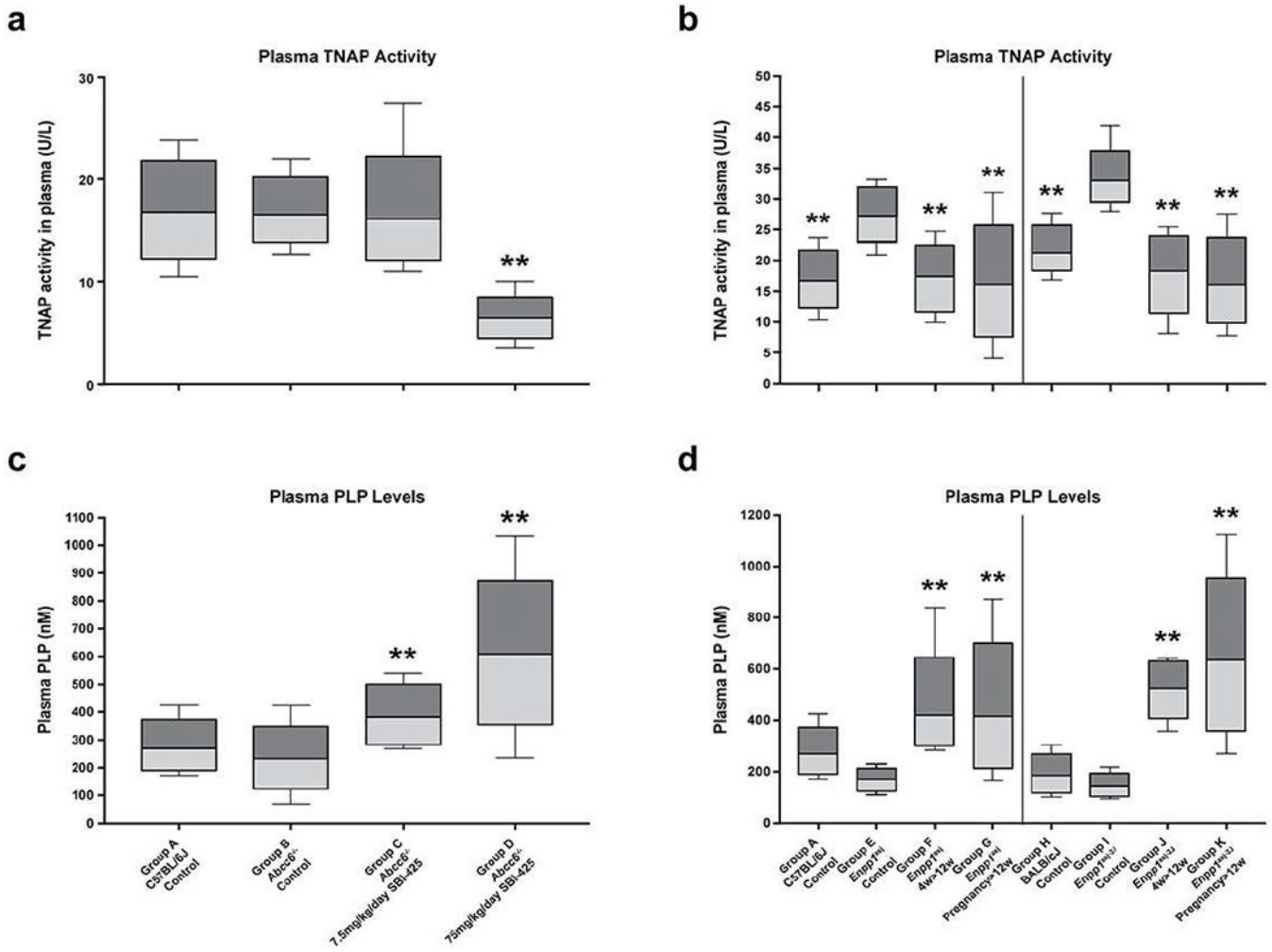

Figure 2. Treatment of mice with SBI-425 resulted in decreased TNAP activity and increased PLP levels in plasma.

Plasma TNAP activities and PLP levels in the *Abcc6*$^{-/-}$ mice (a) and *Enpp1* mutant mice (b; left panel, *Enpp1*^{asj}; right panel, *Enpp1*$^{asj\text{-}2J}$ mice). Treatment with 75 mg/kg/day SBI-425 resulted in reduction of plasma TNAP activity with concomitant increase of PLP levels in the *Abcc6*$^{-/-}$ mice (Group D) as compared to the *Abcc6*$^{-/-}$ control mice (Group B); Note significant increase of plasma TNAP activity in the *Enpp1*^{asj} and *Enpp1*$^{asj\text{-}2J}$ mice (Group E and I) as compared to their respective wild type controls (Group A and H). Treatment with 75 mg/kg/day SBI-425 starting at 4 weeks of age (Group F and J) or in pregnant mothers (Group G and K) resulted in significant reduction of TNAP activities and increase of PLP levels in the progeny when examined at 12 weeks of age. Values were expressed as mean ± SD; n = 7 - 20 mice per group. $^{**}p < 0.01$, compared with *Abcc6*$^{-/-}$ (Group B), *Enpp1*^{asj} (Group E), or *Enpp1*$^{asj\text{-}2J}$ (Group I) mice on control diet.

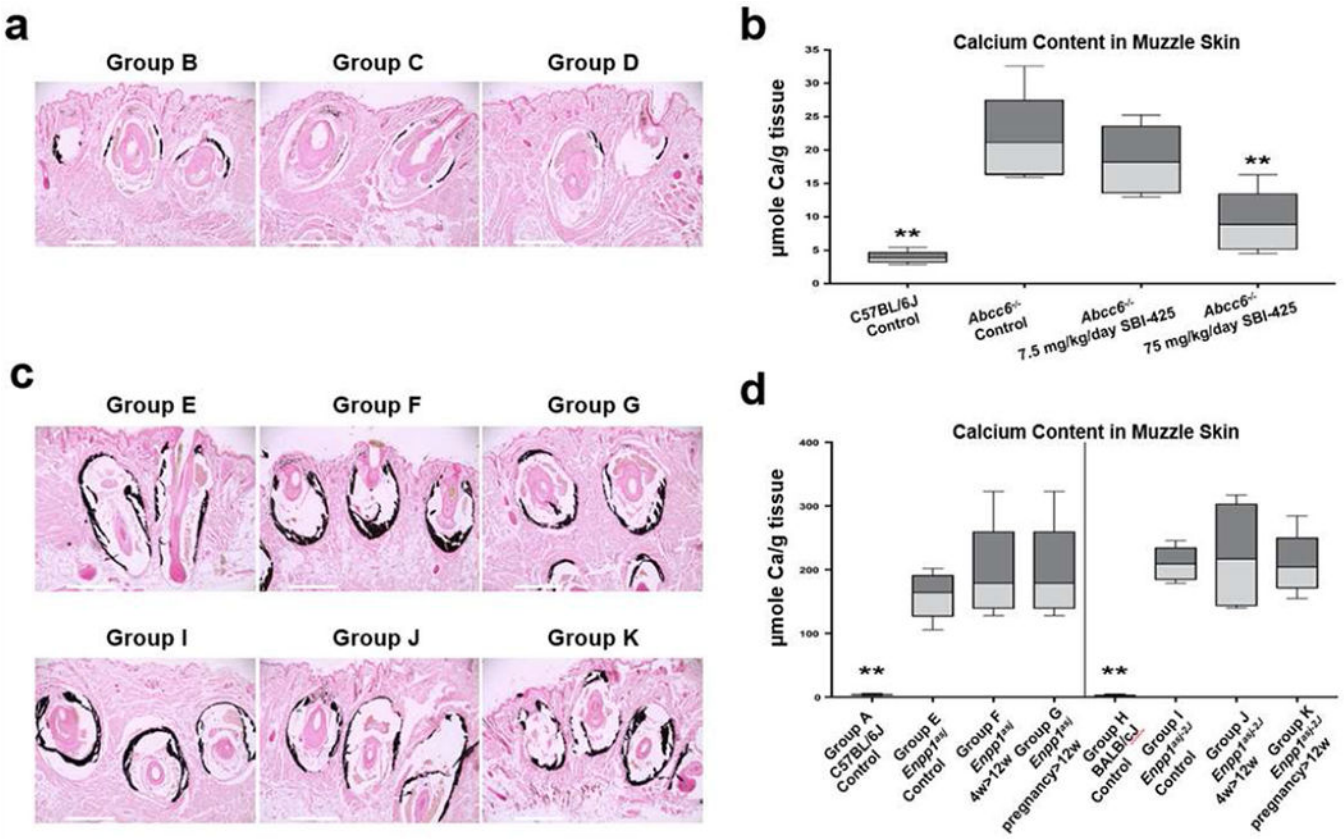

Figure 3. Treatment with SBI-425 attenuated ectopic connective tissue mineralization in *Abcc6*$^{-/-}$ mice but not in *Enpp1*^{asj} and *Enpp1*$^{asj-2J}$ mice.

(a) Tissues were collected from *Abcc6*$^{-/-}$ mice at 12 weeks of age and analyzed by histopathology with von Kossa stains. The *Abcc6*$^{-/-}$ mice treated with 7.5 mg/kg/day SBI-425 (Group C) had similar levels of mineralization in the muzzle skin to that of *Abcc6*$^{-/-}$ control mice (Group B). In contrast, treatment with 75 mg/kg/day SBI-425 revealed marked decrease of mineralization (Group D); (b) The chemical assay of calcium demonstrated significant reduction in the amount of calcium in the muzzle skin in the *Abcc6*$^{-/-}$ mice treated with 75 mg/kg/day SBI-425 (Group D); (c) The *Enpp1*^{asj} mice (upper panel) and *Enpp1*$^{asj-2J}$ mice (lower panel) treated with 75 mg/kg/day SBI-425 postnatally (Group F and J) and in pregnant mothers (Group G and K) had similar levels of mineralization in the muzzle skin to their respective mutant mice on the control diet (Group E and I); (d) The chemical assay of calcium did not reveal differences in the amount of calcium in the muzzle skin in the treated mice. Values were expressed as mean ± SD; n = 7 - 20 mice per group. $^{**}p < 0.01$, compared with *Abcc6*$^{-/-}$ (Group B), *Enpp1*^{asj} (Group E), or *Enpp1*$^{asj-2J}$ (Group I) mice on control diet. Scale bar, 0.4 mm.

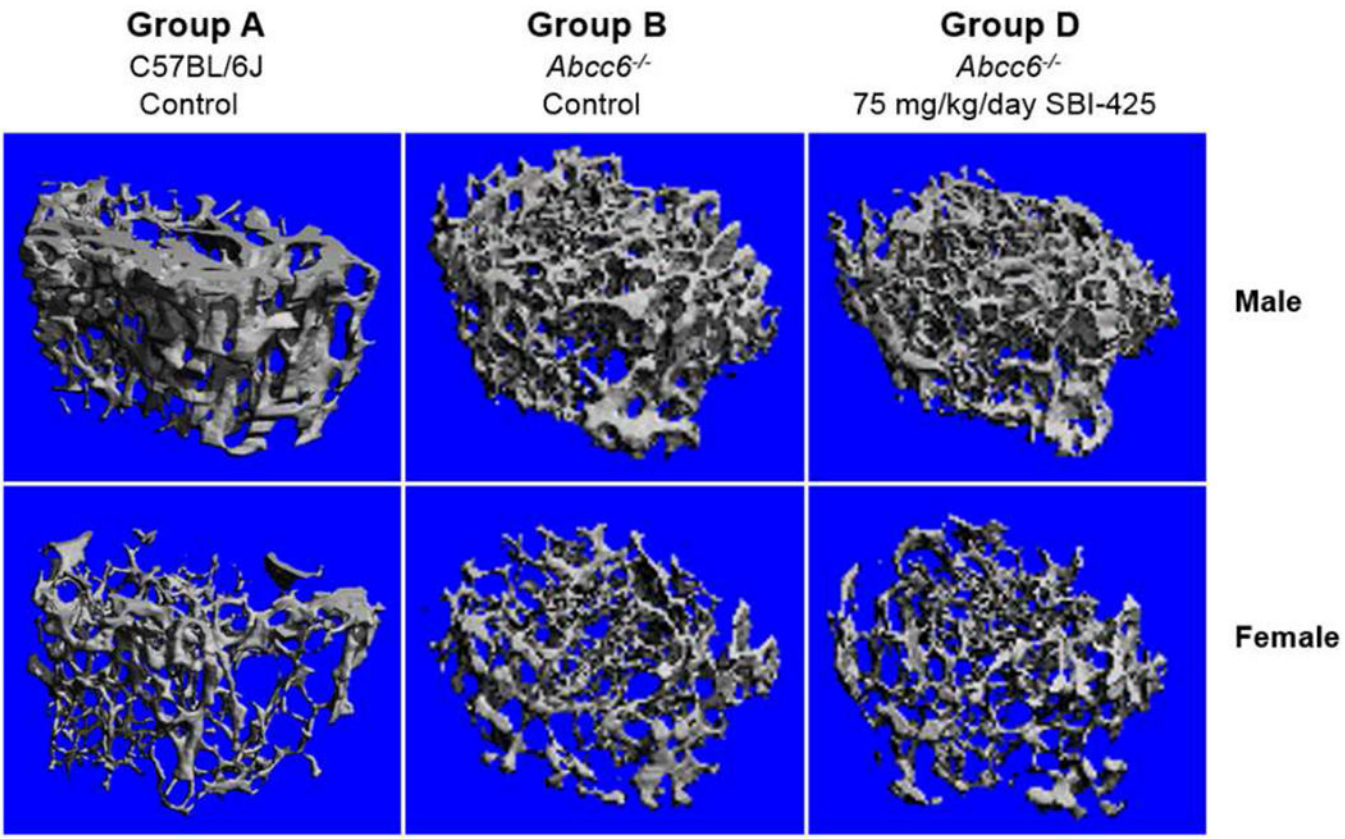

Figure 4. MicroCT analysis does not reveal changes in trabecular bone microarchitecture in the *Abcc6*$^{-/-}$ mice treated with 75 mg/kg/day SBI-425.

Note the distinct differences between male and female mice in each group. Changes were not found in *Abcc6*$^{-/-}$ mice (Group B) compared to wild type C57BL/6J mice (Group A). Treatment with 75 mg/kg/day SBI-425 in the *Abcc6*$^{-/-}$ mice (Group D) did not alter the femoral microarchitecture as compared to *Abcc6*$^{-/-}$ control mice (Group B). n = 3-5 per sex in each group. Their respective quantitative data were detailed in Table 2.

Table 1.

Experimental groups of mice by genotype and treatment *

Group	Genotype	No. of mice examined (M+F)	Treatment	Treatment started > treatment ended (weeks)
Set 1 (*Abcc6*$^{-/-}$ mice)				
A	C57BL/6J	12 (6+6)	Control diet	4 > 12
B	*Abcc6*$^{-/-}$	12 (6+6)	Control diet	4 > 12
C	*Abcc6*$^{-/-}$	12 (6+6)	SBI-425 7.5 mg/kg/day	4 > 12
D	*Abcc6*$^{-/-}$	15 (9+6)	SBI-425 75 mg/kg day	4 > 12
Set 2 (*Enpp1*^{asj} mice)				
E	*Enpp1*^{asj}	11 (6+5)	Control diet	4 > 12
F	*Enpp1*^{asj}	10 (4+6)	SBI-425 75 mg/kg/day	4 > 12
G	*Enpp1*^{asj}	20 (8+12)	SBI-425 75 mg/kg/day	pregnancy > 12
Set 3 (*Enpp1*$^{asj\text{-}2J}$ mice)				
H	BALB/2J	12 (6+6)	Control diet	4 > 12
I	*Enpp1*$^{asj\text{-}2J}$	8 (3+5)	Control diet	4 > 12
J	*Enpp1*$^{asj\text{-}2J}$	7 (3+4)	SBI-425 75 mg/kg/day	4 > 12
K	*Enpp1*$^{asj\text{-}2J}$	11 (4+7)	SBI-425 75 mg/kg/day	pregnancy > 12

* Some mice with desired genotype were placed on either control diet or SBI-425 containing diets at 4 weeks of age and followed for another 8 weeks (4 > 12 weeks). Some pregnant mothers were placed on SBI-425 containing diets during pregnancy and nursing and continuing for the first 12 weeks of postnatal life of the offspring (pregnancy > 12 weeks). The mice were sacrificed at the age of 12 weeks for analysis. M, male; F, female.

Table 2.

Trabecular bone phenotypes of the femurs by microCT analysis

Group[1)]	Sex	BMD (mg/cm^3)	BV/TV (%)	Tb.Th (μm)	Tb.N (1/mm)	Tb.Sp (μm)	SMI	Conn.D (TV/mm^3)
A	M	198.9 ± 70.5	14.6 ± 2.9	37.7 ± 20.2	4.4 ± 0.1	222.7 ± 6.0	2.1 ± 0.8	207.5 ± 106.1
A	F	100.2 ± 13.4	5.8 ± 2.5**	30.6 ± 4.6	3.6 ± 0.2**	277.5 ± 16.0**	2.7 ± 0.5	124.2 ± 54.5
B	M	246.1 ± 12.2	17.8 ± 1.3	44.8 ± 7.7	5.7 ± 0.5	168.4 ± 13.6	1.5 ± 0.1	378.3 ± 118.0
B	F	125.0 ± 24.8**	7.4 ± 2.0**	33.2 ± 3.1*	4.0 ± 0.3**	247.4 ± 22.0**	2.2 ± 0.3**	185.1 ± 52.2*
D	M	210.8 ± 62.2	14.4 ± 5.7	37.9 ± 6.4	5.5 ± 0.8	178.1 ± 23.5	1.6 ± 0.5	363.3 ± 132.5
D	F	150.0 ± 23.6	9.0 ± 2.0	34.5 ± 1.3	4.5 ± 0.4	218.6 ± 21.4*	2.2 ± 0.2	241.4 ± 52.6

1)For a description of different groups, see Table 1.

Abbreviations: M, male; F, female; BMD, bone mineral density; BV/TV, relative bone volume; Tb.Th, trabecular thickness; Tb.N, trabecular number; Tb.Sp, trabecular separation (marrow thickness); SMI, structure model index; Conn.D, connectivity density.

Values are expressed as mean ± SD. N = 3-5 males and females per group.

* $p < 0.05$

** $p < 0.01$, compared to the male mice in each group;

No statistical differences are noted in mice in Group B when compared to sex matched mice in Groups A and D.